Environmental Research Letters

CrossMark

OPEN ACCESS

RECEIVED
10 February 2016

REVISED
21 April 2016

ACCEPTED FOR PUBLICATION
29 April 2016

PUBLISHED
19 May 2016

LETTER

El Niño's impact on California precipitation: seasonality, regionality, and El Niño intensity

Bor-Ting Jong[1,2], **Mingfang Ting**[1] **and Richard Seager**[1]

[1] Lamont-Doherty Earth Observatory, Columbia University, Palisades, NY, USA
[2] Department of Earth and Environmental Sciences, Columbia University, New York, NY, USA

E-mail: borting@ldeo.columbia.edu

Keywords: California precipitation, El Niño, teleconnection

Abstract

California has experienced severe drought in recent years posing great challenges to agricultural production, water resources, and land management. El Niño, as the prime source of seasonal to interannual climate predictability, offers the potential of amelioration of drought in California. Here El Niño's impacts on California winter precipitation are examined, focusing on variations by season, region, and the strength of El Niño using observational data for the period 1901–2010. The El Niño influence on California precipitation strengthens from early to late winter and is stronger in the south than the north. Eight of ten moderate-to-strong El Niños in the late winter put southern California in the wettest tercile and none of these ten events put northern California in the driest tercile. The early to late winter strengthening of the El Niño impact on precipitation occurs even as El Niño weakens and is associated with a strengthening and eastward extending tropical deep convection anomaly allowed by the late winter warming of the climatological mean sea surface temperature over the tropical eastern Pacific.

1. Introduction

As California battles severe drought, it becomes increasingly important to understand the atmospheric and oceanic conditions that could interrupt or even end the drought that began in 2011. Recent researches (Davies 2015, Hartmann 2015, Seager *et al* 2015, Watson *et al* 2016) indicate that the current drought is associated, to a significant degree, with warm sea surface temperature anomalies (SSTA) in the western tropical Pacific Ocean and, some argue, cool SSTA in the central to eastern equatorial Pacific. As the SSTA pattern evolved during the 2015/2016 El Niño event, an important question emerged as to the likelihood of El Niño moderating drought conditions. After all, El Niño, the most significant mode of climate variability and the only reliable source of seasonal to interannual prediction, imposes a major control on western North America climate (e.g. Schonher and Nicholson 1989, Cayan and Redmond 1994, Mo and Higgins 1998, Andrews *et al* 2004, Schubert *et al* 2008, Seager and Hoerling 2014). Since California is one of the largest economies in the world and a world leader in agricultural production, improved understanding of El Niño's impact on California precipitation has great economic and societal value.

During an El Niño, a low-frequency Rossby wave-train, forced by the positive SSTA and enhanced deep convection in the tropical Pacific, propagates from the equator to extratropical regions over the North Pacific and North America (e.g. Rasmusson and Wallace 1983, Trenberth *et al* 1998), influencing climate in remote regions via well-known 'teleconnections'. The large-scale anomalous atmospheric circulation patterns impact the weather across all of North America, leading to wetness in the southeastern US during El Niño winters (e.g. Ropelewski and Halpert 1986, 1996, Livezey *et al* 1997, Mason and Goddard 2001, Chiodi and Harrison 2013) as well as a dry north-wet south pattern across western North America (e.g. Livezey *et al* 1997, Dettinger *et al* 1998). However, the influence of El Niño conditions on western North American rainfall, particularly California, is not robust and shows substantial variability among different historical events (Yarnal and Diaz 1986).

Two of the most prominent mid-latitude responses to El Niños are the deepening of the Aleutian Low (e.g. Bjerknes 1969, Schonher and Nicholson 1989) and the strengthening and southward shift of the subtropical jet over the North Pacific (Trenberth *et al* 1998). Both conditions could lead to a southward shifted storm track and cause anomalous wetness at the US southwest coast (Seager *et al* 2010). On a regional scale, however, the precise location and timing of the precipitation increase can be extremely sensitive to the longitudinal and latitudinal position and strength of the low pressure anomaly, which determines how circulation anomalies may steer storms towards the US west coast (Yarnal and Diaz 1986). For example, in California, if the low pressure anomaly is located right off the west coast, the entire state tends to be wetter during an El Niño winter; while if the low anomaly is located further to the west or north, precipitation may actually reduce in California (e.g. Schonher and Nicholson 1989, Ely *et al* 1994).

Furthermore, the impact of El Niño on California rainfall varies from north to south (Schonher and Nicholson 1989, Cayan *et al* 1999, Andrews *et al* 2004, Schubert *et al* 2008). About two-thirds of the total winter precipitation in California falls on the windward side of the northern California Sierra Nevada mountain range (Dettinger *et al* 2011), but it is southern California, the relatively dry part of the state, that has the strongest relationship with El Niño.

Though the above studies pointed out the differences of El Niño's impact in northern and southern California, most of them focused on the relationships by using winter half year or annual data. However, the change in El Niño impacts throughout the winter season and the role of El Niño intensity have not been fully examined and well-documented. In this study, we focus on quantifying El Niño's impact on California precipitation based on historical observations of precipitation, SST, and atmospheric circulations. The goal is to determine the dependence of the El Niño—California precipitation relationship on timing (early versus late winter), region (northern versus southern California), and the strength of the El Niño SSTA. Such information will be of use in seasonal forecasting for California, including the alleviation and/or termination of drought conditions.

2. Data and method

In this study, the relationships between SSTA in the Niño 3.4 region (120° W–170° W, 5° S–5° N) and northern and southern California winter precipitation (November–April) from 1900/01 to 2009/10 are examined. Sea surface temperature data are taken from the extended reconstructed sea surface temperature (ERSST) version 3b from the National Oceanographic and Atmospheric Administration (NOAA) (Smith *et al* 2008). ERSST provides monthly SST data from 1895 with 2° × 2° spatial resolution. Here, the trend from 1900/01 to 2009/10 of Niño3.4 SSTA (0.065 °C/10 year for November, December, and January (NDJ); 0.053 °C/10 year for February, March, and April (FMA)) is removed to isolate the interannually varying component. To be consistent, all the variables used in this research have been linearly de-trended and the trend is removed for each three-month season. The California precipitation data are taken from the Global Precipitation Climatology Centre (GPCC, Full Data Product version6) that provides monthly gridded precipitation from 1901 to 2010 with 0.5° × 0.5° spatial resolution (Schneider *et al* 2013). The state of California is divided into northern and southern parts based on the characteristics of the climatological winter precipitation (figure 1(a)) as well as the correlations between precipitation and de-trended Niño3.4 SSTA (figure 1(b)). Here, northern California is defined as the region within 124° W–118° W, 36° N–42° N, while southern California is within 122° W–114° W, 32° N–36° N (see the two black boxes in figures 1(a) and (b)).

The atmospheric circulation data for 200 hPa geopotential height are taken from the NOAA 20th Century reanalysis version 2c (Compo *et al* 2015). The monthly data are available from 1851 to 2014 with 2° × 2° spatial resolution. To understand the El Niño teleconnection, global precipitation, near-surface moist static energy (MSE) and convective available potential energy (CAPE) from 1979/80 to 2009/10 are also used in this research. Monthly global precipitation data are obtained from the Global Precipitation Climatology Project (GPCP, version 2) (Adler *et al* 2003), from January 1979 to the present with a spatial resolution of 2.5° × 2.5°. Monthly MSE and CAPE data are derived from European Center for Medium-Range Weather Forecasts interim reanalysis dataset (ERA-Interim) from January 1979 to November 2015 with a spatial resolution of 1.5° × 1.5° (Dee *et al* 2011). The identification of El Niño and La Niña years is based on the 'Oceanic Niño Index (ONI)', derived from the 3 month running mean of Niño3.4 SSTA, relative to a centered 30 year climatology updated every 5 years. El Niño events are defined when the ONI reaches the threshold of +0.5 °C for at least 5 consecutive 3 month means (see the NOAA Climate Prediction Center website: http://www.cpc.ncep.noaa.gov/products/analysis_monitoring/ensostuff/ensoyears.shtml for a complete description). In this study, the definition of weak and moderate-to-strong El Niños is based on the strength of the de-trended Niño3.4 SSTA. Weak (moderate-to-strong) El Niños are defined as the Niño3.4 SSTA between 0.5 °C and 1 °C (more than 1 °C) for the corresponding season.

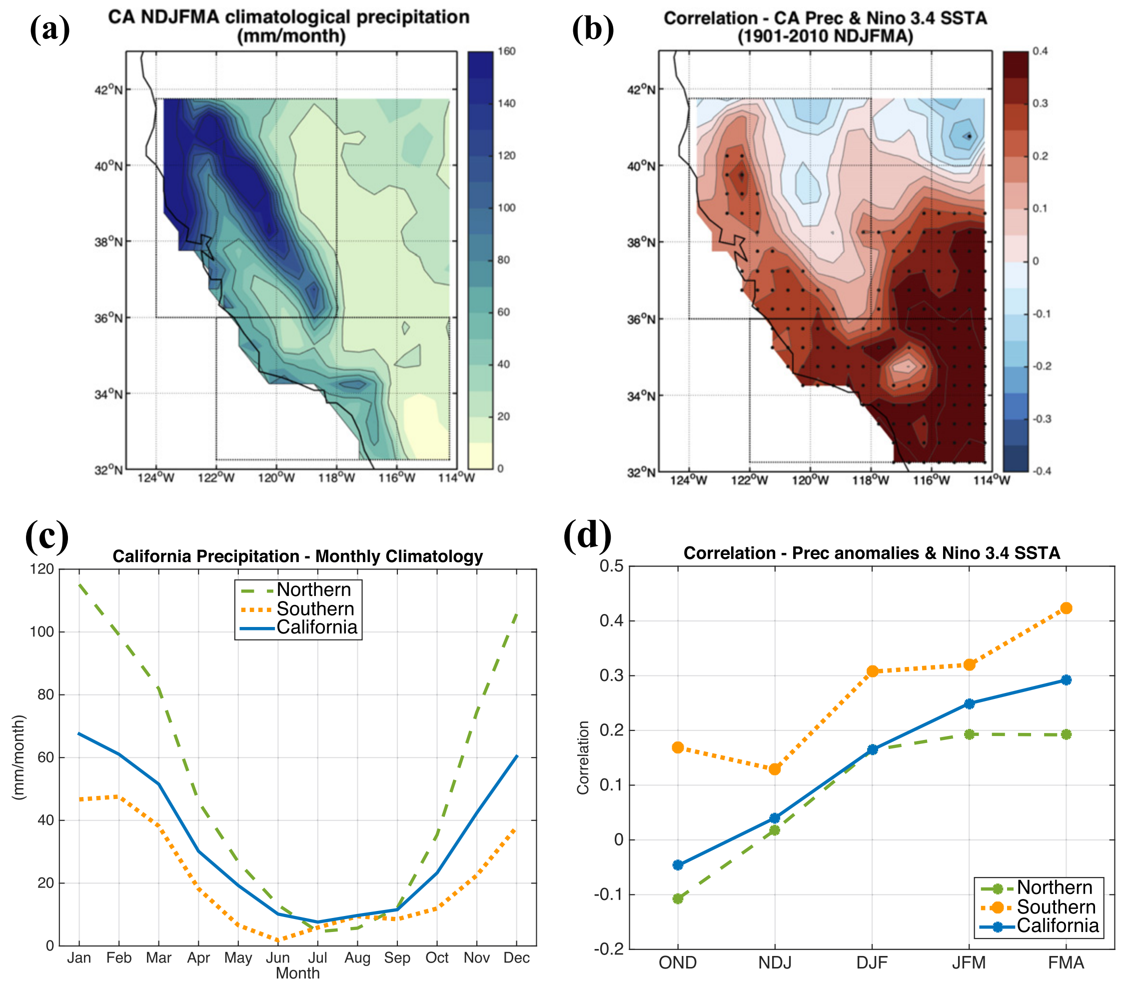

Figure 1. (a) California region climatological precipitation for the 6 month cold season (NDJFMA, 1900/01–2009/10) in units of mm/month. The boxes indicate the areas of northern and southern California used in this research. (b) Correlation coefficients between precipitation and de-trended Niño3.4 SSTA (NDJFMA, 1900/01–2009/10). Stippling denotes 95% significance. (c) Monthly climatology of precipitation averaged for the California region (blue solid line), northern California (green dashed line), and southern California (orange dotted line) in units of mm/month. (d) Correlation coefficients between 3 month running mean de-trended Niño3.4 SSTA and 3 month running mean precipitation in California region (blue solid), northern (green dashed), and southern (orange dotted) California.

3. Results

The seasonal cycles of the monthly precipitation over the entire state and the northern and southern parts of California are shown in figure 1(c). There is a clear peak in total precipitation in winter months, from December to February. Northern California receives more than double the amount of precipitation of southern California. Three-month running mean correlations between California precipitation and the de-trended Niño3.4 SSTA are shown in figure 1(d). There is an almost linear increase in correlation from October, November and December (OND) and February, March, and April (FMA) for all three regions. The precipitation in northern California is only weakly influenced by El Niño Southern Oscillation (ENSO, including El Niño and La Niña), as shown in figure 1(d), possibly due to large internal atmospheric variability in northern California caused by mid-latitude weather systems. Although the west portion of northern California shows a coherent region of significant correlation with ENSO, the relation is not as strong as in southern California, where the correlation is largely significant throughout the winter season.

To examine further the relationship between California winter precipitation and El Niño on a year-to-year basis, as well as the difference in the relationship for northern and southern California during early and late winters, figure 2 shows scatter plots for precipitation anomalies in percent of climatology in northern and southern California as a function of the Niño3.4 SSTA. The percentages, instead of the absolute values, are used here because the distribution of precipitation is extremely uneven across the state, as shown in figure 1(a). The percent of climatology is defined here based on the area-averages of precipitation anomaly and climatology. We also calculated the precipitation percent anomaly at each grid point first and then area-averaged the percentages over northern and southern

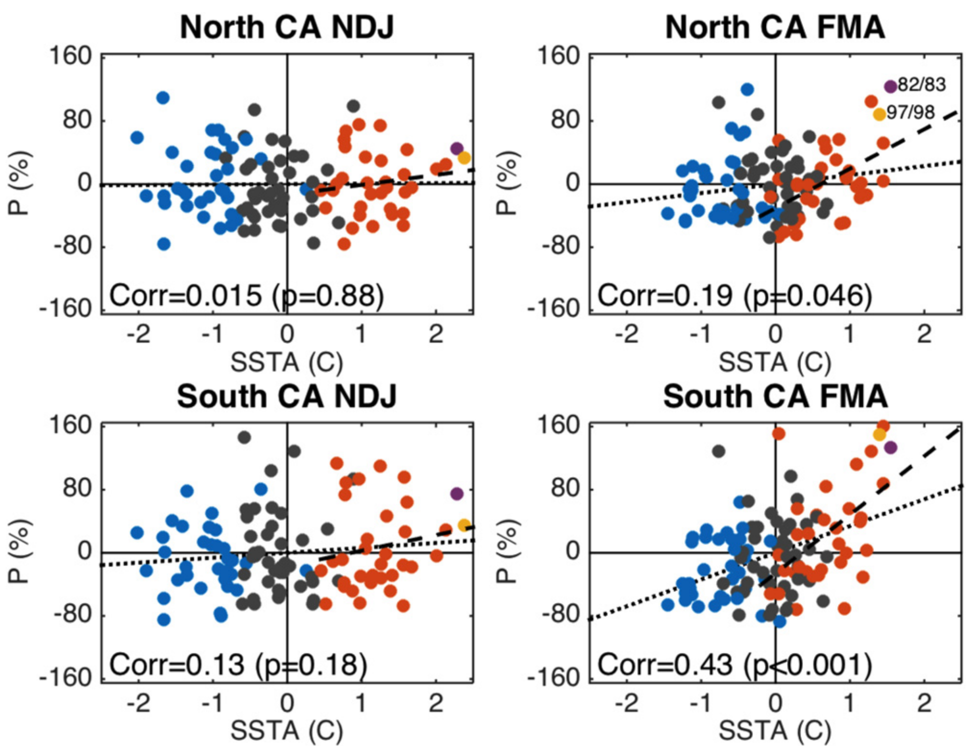

Figure 2. De-trended precipitation anomaly (% of climatology) as a function of de-trended Niño3.4 SSTA for northern (upper) and southern (bottom) California in early (NDJ; left) and late (FMA; right) winter from 1900/01 to 2009/10. Red, black, and blue dots denote El Niño, neutral, and La Niña years, respectively. The two strongest El Niño events on record (1982/83 and 1997/98) are indicated as purple and yellow dots, respectively. Dashed lines are the best fits for El Niño events only.

California. The results in figure 2 are insensitive to how the percent of climatology is calculated. The colors in figure 2 indicate El Niño (red), La Niña (blue) and neutral (black) years according to the NOAA definition as explained in section 2. In early winter (NDJ), the Niño3.4-precipitation relationships are very weak for both northern and southern California, although the strongest El Niño events tend to have above normal precipitation in both regions. In contrast, in late winter (FMA), the relationships strengthen in both northern and southern California. While the correlation in northern California is weak (0.19), it is significant at the 5% level and, furthermore, precipitation anomalies are all above normal for the five most intense El Niño events. In southern California, the correlation is highly significant (0.43), with the strong El Niño events having between 80% and 160% above climatological normal precipitation. Figure 2 also indicates the asymmetry of ENSO's impact on precipitation for northern and southern California. In late winter, the correlation between precipitation anomalies and Niño3.4 SSTA for El Niño events only (dashed lines in figure 2) is 0.50 ($p = 0.0025$) in northern California and 0.53 ($p = 0.0014$) in southern California, both are highly significant. Compared to the correlations for all years (shown in figure 2), northern California has a high tendency to be wet during an El Niño, but not necessarily dry during La Niña. The asymmetry also exists in southern California, although to a lesser extent. The lack of significant impact of the La Niña events on California precipitation may be related to the fact that suppressed convection and the associated atmospheric teleconnection patterns tend to be located further to the west, and away from the North American west coast, for La Niña compared to El Niño (Hoerling *et al* 1997).

To understand the difference between El Niño's impacts on early and late winter California precipitation, figure 3 shows the composites of 200 hPa geopotential height anomalies (contours) and SSTA (shading) for moderate-to-strong El Niños and weak El Niños for early and late winter. The corresponding California precipitation anomalies in percent of climatology are also shown. In all four cases, there is a low-pressure anomaly over the northern North Pacific, a high anomaly over Canada and another low over the Southeastern US, consistent with the well-known Pacific North American (PNA) teleconnection pattern (Horel and Wallace 1981). In the moderate-to-strong El Niño composites, however, the intensity of the PNA pattern increases in late winter even though the tropical Pacific SSTA decreases slightly (top panels in figure 3). The differences of 200 hPa height in late and early winter are statistically significant at 95% confident interval over the eastern North Pacific and the US west coast (figure not shown). The anomalous Aleutian Low for late winter is almost double the

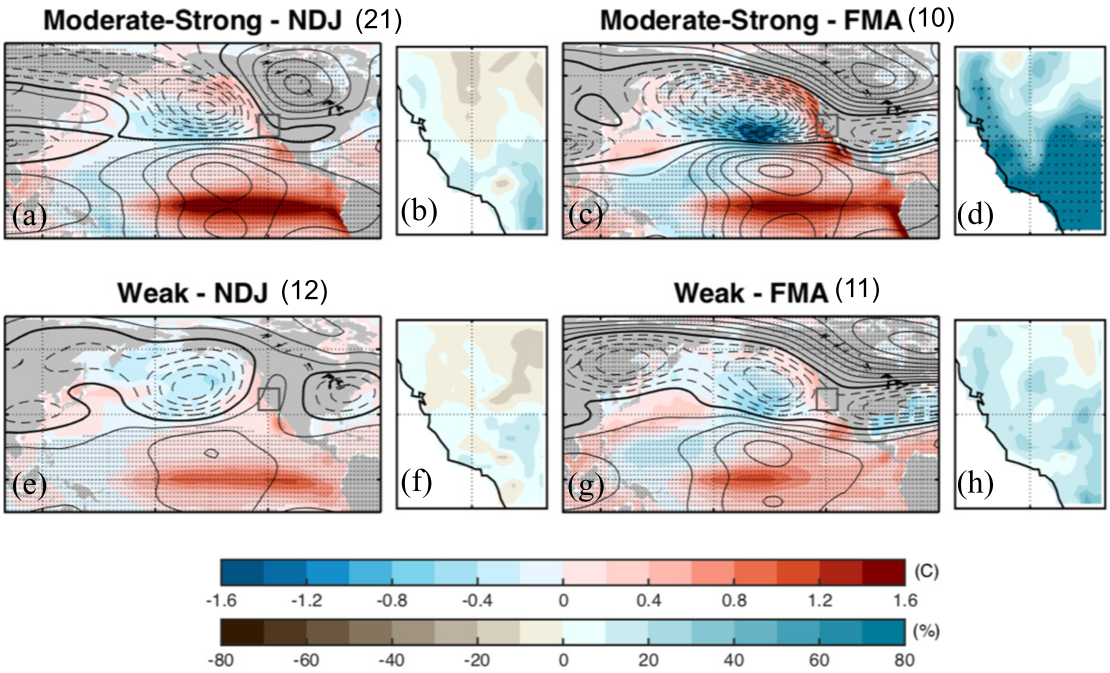

Figure 3. Composites of (a), (c), (e) and (g) 200 hPa height anomalies (contour, interval: 10 m), SSTA (ocean) and (b), (d), (f), (h) precipitation anomalies (% of climatology) for moderate-to-strong (top) and weak (bottom) El Niños in early (left) and late (right) winters during 1900/01 to 2009/10. All the anomalies here are de-trended. The plotting region for (b), (d), (f), (h) is within 124° W–114° W, 32° N–41° N, indicated by the boxes in (a), (c), (e), (g). Stippling regions in (a), (c), (e), (g) indicate the 95% significance for 200 hPa height variations. Stippling regions in (b), (d), (f), (h) indicate the 95% significance for precipitation variations. The definition of weak and moderate-to-strong El Niños is described in section 2. The numbers of El Niño events for each case are indicated in the titles.

amplitude of that for early winter while the Niño3.4 SSTA decreased from 1.52 °C to 1.29 °C (table 1). Correspondingly, the precipitation anomaly in northern (southern) California is more than 10 (8) times larger in late winter than in early winter (see table 1). For the weak events (lower panels), however, the seasonal dependence is less striking although late winter does show lower heights over California and a stronger precipitation response (table 1).

The possible cause of the apparent nonlinear relationship between SSTA amplitude and teleconnection strength in figure 3 for early and late winter may be the warmer equatorial Pacific SST basic state in late winter. That is, even though, during an El Niño event, the SSTA weakens from early to late winter, the smaller anomalies in late winter are imposed on a warmer climatological SST, which leads to a more favorable environment for deep convection. To investigate this, figure 4 shows the composites of precipitation anomalies (shaded) and total SST (contours) in early and late winters for the moderate-to-strong El Niño events that have occurred since satellite observations became available. The SSTA composites for this period are similar to those in figure 3 (top panels). While, the Niño3.4 SSTA amplitude is 1.57 °C for early winter and 1.39 °C for late winter (table 1), the composites of precipitation anomalies show a much stronger late winter signal that also extends further to the east of the corresponding location in early winter. The total SST composites show that, in late winter, the warmest

Table 1. Average de-trended Niño3.4 SSTA and northern and southern California precipitation anomalies (in % of climatology) for moderate-to-strong (upper) and weak (lower) El Niños in early and late winters during 1900/01 to 2009/10. The anomalies for moderate-to-strong El Niños during 1979/80 to 2009/10 are shown in parentheses. Italic (asterisk) numbers indicate the 90% (95%) significance of variations.

	Niño3.4 SSTA (°C)		CA precip anomalies (%)			
	NDJ	FMA	NDJ		FMA	
Moderate-strong	*1.52**	*1.29**	N	3% (12%)	N	*33%* (50%)
	(*1.57**)	(*1.39**)	S	10% (25%)	S	*83%** (81%)
Weak	*0.79**	*0.77**	N	1.72%	N	12.94%
			S	5.05%	S	13.34%

region (indicated by the 28 °C isotherm, thick lines in figure 4) extends further east, which enhances the deep convection and precipitation anomalies in the central and eastern Pacific.

To further examine the characteristics of the environment for deep convection, figure 5 shows the latitudinally averaged 1000 hPa MSE, CAPE and precipitation between 10° N and 15° S for early and late winters during moderate-to-strong El Niños. The near-surface entropy (MSE) and CAPE are measures of the strength of instability that deep convection removes. In the central to eastern Pacific (around

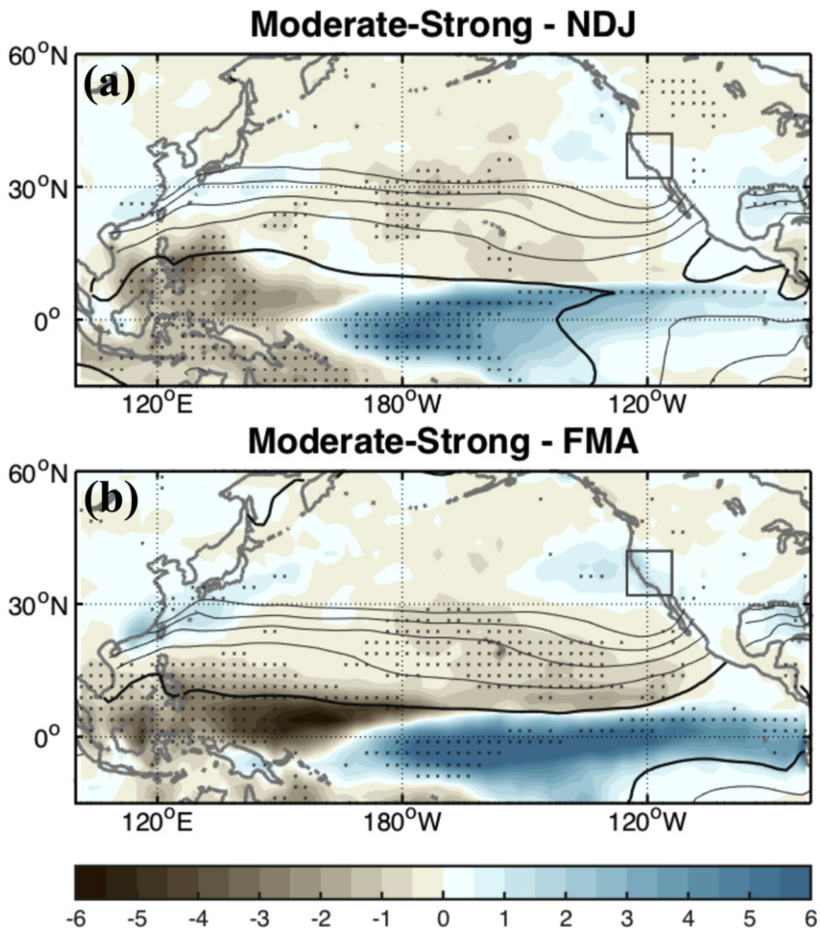

Figure 4. Composites of GPCP precipitation anomalies (shaded, unit: mm/day) and SST (contour, interval: 1 °C) for moderate-to-strong El Niño in (a) early and (b) late winters during 1979/80 to 2009/10. Thick contours indicate SST 28 °C isotherm. Stippling regions indicate 95% significance for precipitation variations. All the variables used here are de-trended.

150° W–80° W), near-surface MSE and CAPE (figures 5(a), (b)) are larger in late winter than in early winter, indicating a more unstable environment favorable to deep convection, consistent with the larger precipitation composites in late winter (figure 5(c)). The results in figures 4 and 5 support the hypothesis that stronger teleconnection patterns in late winter occur due to stronger and more eastward-spread tropical heating anomalies. This is a consequence of warmer climatological SST conditions in the eastern tropical Pacific in late winter than early winter allowing a smaller SSTA to cross the threshold for deep convection. Further idealized modeling experiments are needed to fully understand the differences in early and late winter teleconnections, the dynamical mechanisms behind it, and the possible additional contribution from the tropical-wide warming that follows the peaking of the El Niño.

4. Discussions and conclusions

The seasonality, regionality and dependence on El Niño intensity of California rainfall anomalies have important implications for seasonal prediction of El Niño's impacts. Dividing the climatological precipitation distribution into terciles, table 2 shows the number of moderate-to-strong and weak El Niño events that fell into each tercile, for northern and southern California and for early and late winter, as well as the associated precipitation anomaly, expressed as percent of climatology for each tercile. This provides overall information about the relationship between El Niño and California precipitation. During early winter, in both northern and southern California, there is no clear preference for El Niños to be in the wettest tercile. However, in late winter, eight of ten moderate-to-strong El Niño events put southern California in the wettest tercile. For northern California, none of these ten events put northern California in the driest tercile, six were in the middle tercile and four in the upper tercile. In other words, with regard to season, El Niño's impacts are likely to be stronger in late winter than in early winter; and, in terms of region, southern California has a greater chance of wet winters during an El Niño than northern California. Further, only a relatively strong El Niño is likely to bring heavy precipitation across the entire state. In summary, a moderate-to-strong El Niño in the late winter can

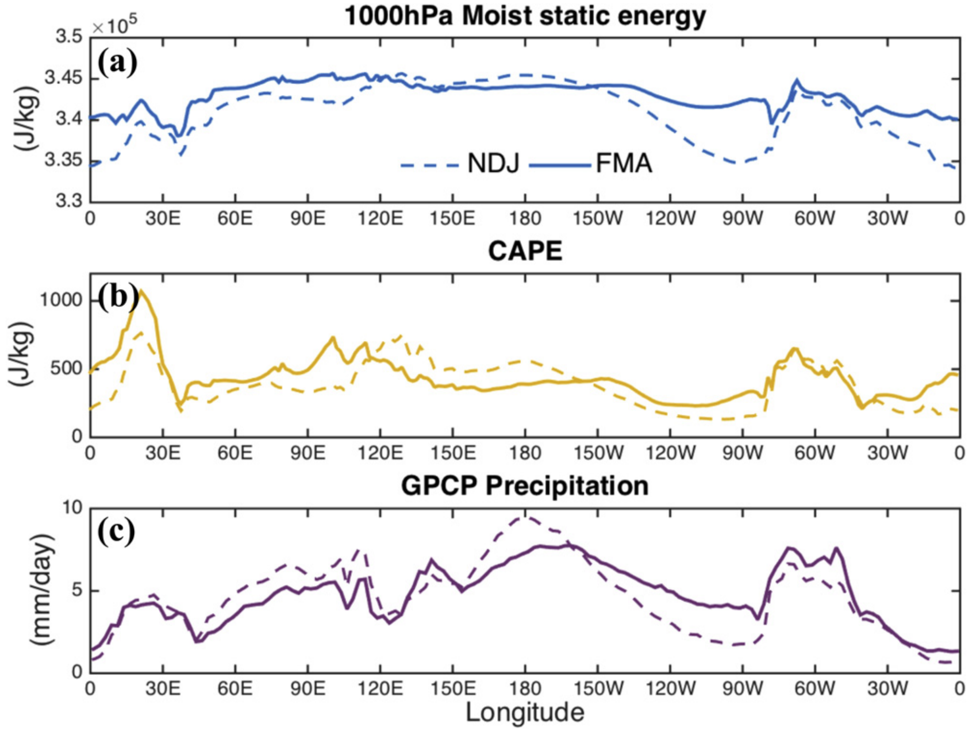

Figure 5. Composites of latitudinal average (a) 1000 hPa moist static energy, (b) convective available potential energy (CAPE), and (c) GPCP precipitation between 10° N and 15° S for moderate-to-strong El Niño in early (dashed lines) and late (solid lines) winters during 1979/80 to 2009/10.

Table 2. Precipitation anomaly (% of climatology) of each precipitation tercile in northern (top) and southern (bottom) California during moderate-to-strong and weak El Niños in early (left) and late (right) winters. The number of events for each category is shown in parentheses. (For instance, for the past 10 moderate-to-strong El Niño during late winter, 1 had below normal precipitation southern California; 1 had a normal precipitation; 8 were associated with above normal precipitation. These 8 winters had precipitation 107% above climatology on average.) Italic (asterisk) numbers indicate statistically significant at 90% (95%) confidence using Monte Carlo bootstrapping method.

		NDJ			FMA		
		Lower	Middle	Upper	Lower	Middle	Upper
North	Strong El Niño	−43% (5)	−2% (9)	42% (7)	−(***0****)	−7% (6)	92% (4)
	Weak El Niño	−46% (5)	0% (3)	63% (4)	−49% (2)	6% (3)	37% (***6****)
South	Strong El Niño	−42% (5)	−10% (7)	55% (9)	−35% (***1***)	9% (1)	107% (***8****)
	Weak El Niño	−48% (6)	−9% (2)	92% (4)	−71% (***1***)	−9% (5)	53%(5)

make southern California precipitation very likely to be in the upper tercile and make northern California precipitation very unlikely to be in the lower tercile, while a weak El Niño or a moderate-to-strong El Niño in early winter cannot be relied upon to favor a wet winter in California.

El Niño's impact on California late winter precipitation is associated with the strengthening of the teleconnection from early to late winter even though the tropical Pacific SSTA decreases slightly. This nonlinearity between SSTA and teleconnection response is possibly caused by a stronger and more eastward extended tropical diabatic heating in late winter due to a warmer climatological mean SST over the tropical eastern Pacific. Further modeling experiments are needed to quantitatively determine the differing atmospheric responses to early and late winter El Niño forcing.

During 2011/12–2014/15, California experienced the driest four successive winters since 1895 (Williams *et al* 2015). The accumulated precipitation deficit for the 4 year period reached 148% in northern California and 195% in southern California of the winter precipitation climatology, which means a very strong El Niño like 1982/83 or 1997/98 might be able to remove the statewide accumulated precipitation deficit within one winter (figure 2). The 2015/16 El Niño, as one of the strongest El Niño events in recent history, is thought to have contributed to several severe storms to California in December 2015 and January 2016, causing serious flash flooding and landslides in southern California. According to the analysis here, the El

Niño impact would have been expected to strengthen after January 2016 even as the El Niño weakens, making significant drought alleviation probable. It will be interesting to see if the El Niño of 2015/16 impact on California precipitation conformed to expectations or, if not, why not.

Acknowledgments

This work was supported by NSF awards AGS-1401400 and AGS-1243204 and NOAA Awards NA14OAR4310232 and NA14OAR4310223. The ERSST, GPCC and GPCP data used in this study are downloaded from the IRI/LDEO Climate Data Library. The ERA-Interim (http://apps.ecmwf.int/archive-catalogue/?class=ei) and 20th Century reanalysis (www.esrl.noaa.gov/psd/data/gridded/data.20thC_ReanV2c.html) data were downloaded directly from the corresponding website. We would like to thank Naomi Henderson for her help with downloading the reanalysis data.

References

Adler R F *et al* 2003 The version-2 global precipitation climatology project (GPCP) monthly precipitation analysis *J. Hydrometeorl.* **4** 1147–67

Andrews E D, Antweiler R C, Neiman P J and Ralph F M 2004 Influence of ENSO on flood frequency along the California coast *J. Clim.* **17** 337–48

Bjerknes J 1969 Atmospheric teleconnections from the equatorial Pacific *Mon. Weather Rev.* **97** 163–72

Cayan D R and Redmond K T 1994 ENSO influences on atmospheric circulation and precipitation in the western United States *10th Annual Pacific Climate (PACLIM) Workshop (Pacific Grove, CA)* pp 5–26

Cayan D R, Redmond K T and Riddle L G 1999 ENSO and hydrologic extremes in the western United States *J. Clim.* **12** 2881–93

Chiodi A M and Harrison D E 2013 El Niño impacts on seasonal US atmospheric circulation, temperature, and precipitation anomalies: the OLR-event perspective *J. Clim.* **26** 822–37

Compo G P *et al* 2015 NOAA/CIRES Twentieth Century Global Reanalysis Version 2c (http://dx.doi.org/10.5065/D6N877TW) Research Data Archive at the National Center for Atmospheric Research, Computational and Information Systems Laboratory, Boulder, CO (updated yearly) (accessed 22 March 2016)

Davies H C 2015 Weather chains during the 2013/2014 winter and their significance for seasonal prediction *Nat. Geosci.* **8** 833–7

Dee D P *et al* 2011 The ERA-Interim reanalysis: configuration and performance of the data assimilation system *Q. J. R. Meteorol. Soc.* **137** 553–97

Dettinger M D, Cayan D R, Diaz H F and Meko D M 1998 North-south precipitation patterns in western North America on interannual-to-decadal timescales *J. Clim.* **11** 3095–111

Dettinger M D, Ralph R M, Das T, Neiman P J and Cayan D R 2011 Atmospheric rivers, floods, and the water resources of California *Water* **3** 455–78

Ely L L, Enzel Y and Cayan D R 1994 Anomalous North Pacific atmospheric circulation and large winter floods in the southwestern United States *J. Clim.* **7** 977–87

Hartmann D L 2015 Pacific sea surface temperature and the winter of 2014 *Geophys. Res. Lett.* **42** 1894–902

Hoerling M P, Kumar A and Zhong M 1997 El Niño, La Niña, and the nonlinearity of their teleconnections *J. Clim.* **10** 1769–86

Horel J D and Wallace J M 1981 Planetary-scale atmospheric phenomena associated with the Southern oscillation *Mon. Weather Rev.* **109** 813–29

Livezey R E, Masutani M, Leetmaa A, Rui H, Ji M and Kumar A 1997 Teleconnective response of the Pacific-North American region atmosphere to large central Pacific SST anomalies *J. Clim.* **10** 1787–820

Mason S and Goddard L 2001 Probabilistic precipitation anomalies associated with ENSO *Bull. Am. Meteorol. Soc.* **82** 619–38

Mo K and Higgins R W 1998 Tropical influences on California precipitation *J. Clim.* **11** 412–30

Rasmusson E M and Wallace J M 1983 Meteorological aspects of the El Niño/Southern Oscillation *Science* **222** 1195–202

Ropelewski C F and Halpert M S 1986 North American precipitation and temperature patterns associated with the El Niño Southern Oscillation (ENSO) *Mon. Weather Rev.* **114** 2352–62

Ropelewski C F and Halpert M S 1996 Quantifying Southern oscillation-precipitation relationships *J. Clim.* **9** 1043–59

Schneider U, Becker A, Finger P, Meyer-Christoffer A, Ziese M and Rudolf B 2013 GPCC's new land surface precipitation climatology based on quality-controlled in situ data and its role in quantifying the global water cycle *Theor. Appl. Climatol.* **115** 15–40

Schonher T and Nicholson S E 1989 The relationship between Califonia rainfall and ENSO events *J. Clim.* **2** 1258–69

Schubert S D, Chang Y, Suarez M J and Pegion P J 2008 ENSO and wintertime extreme precipitation events over the contiguous United States *J. Clim.* **21** 22–39

Seager R, Hoerling M, Schubert S, Wang H, Lyon B, Kumar A, Nakamura J and Henderson N 2015 Causes of the 2011–2014 California drought *J. Clim.* **28** 6997–7024

Seager R and Hoerling M P 2014 Atmosphere and ocean origins of North American drought *J. Clim.* **27** 4581–606

Seager R, Naik N, Ting M, Cane M A, Harnik N and Kushnir Y 2010 Adjustment of the atmospheric circulation to tropical Pacific SST anomalies: variability of transient eddy propagation in the Pacific-North America sector *Q. J. R. Meteorol. Soc.* **136** 277–96

Smith T M, Reynolds R W, Peterson T C and Lawrimore J 2008 Improvements NOAA's historical merged land-ocean surface temperature analysis (1880–2006) *J. Clim.* **21** 2283–96

Trenberth K E, Branstator G W, Karoly D, Kumar A, Lau N and Ropelewski C 1998 Progress during TOGA in understanding and modeling global teleconnections associated with tropical sea surface temperature *J. Geophys. Res.* **103** 291–324

Watson P A G, Weisheimer A, Knight J R and Palmer T N 2016 The role of the tropical West Pacific in the extreme northern hemisphere winter of 2013/14 *J. Geophys. Res. Atmos.* **121** 1698–714

Williams A P, Seager R, Abatzoglou J T, Cook B I and Smerdon J E 2015 Contribution of anthropogenic warming to the 2012–2014 California drought *Geophys. Res. Lett.* **42** 6819–28

Yarnal B and Diaz H F 1986 Relationships between extremes of the Southern oscillation and the winter climate of the anglo-American Pacific coast *J. Climatol.* **6** 197–219